Al-Kitab Journal for Pure Sciences (2025); 9(2):154-168.
https://doi.org/10.32441/kjps.09.02.p10

Al-Kitab Journal for Pure Sciences
ISSN: 2617-1260 (print), 2617-8141(online)
https://isnra.net/index.php/kjps

Assessing The Environmental Quality of Kirkuk City and Taza District Based on Pressure-State-Response Framework for Winter 2023 Using Remote Sensing and GIS

Sundus Mohammed Azeez*, Muntadher Aidi Shareef, Fawzi Mardan Omer

Surveying/ Engineering Technical College- Kirkuk/ Northern Technical University, Mosul, Iraq

*Corresponding Author: Sundus.mohammedgs@ntu.edu.iq

Citation: Azeez SM, Shareef MA, Omer FM. Assessing The Environmental Quality of Kirkuk City and Taza District Based on Pressure-State-Response Framework for Winter 2023 Using Remote Sensing and GIS. Al-Kitab J. Pure Sci. [Internet]. 2025 Sep. 06;9(2):154-168. DOI: https://doi.org/10.32441/kjps.09.02.p10.

KeywordsEco-Environment, Ecologic Index, PSR Framework, Response Indicator, Sentinel-2.

Article History

Received	03 Aug.	2024
Accepted	26 Nov.	2024
Available online	06 Sep.	2025

Abstract:

Evaluating a region's Ecological Environment Quality (EEQ) is an essential factor in deciding its urbanization and sustainable development rate. This study aims to find the Ecological Index (EI). It evaluates it using the widely used Pressure-State-Response (PSR) framework based on a set of statistical and remote sensing indices in Kirkuk City and Taza district. Sentinel-2 satellite images were used to obtain 12 indicators that offer a foundation for sustainable development decision-making for Kirkuk City and Taza District during the winter of 2023. The finding reveals that the ecological condition is healthy in winter due to the atmospheric conditions and the social and economic activities. It presents the main relation between environmental health and human activities.

Keywords: Eco-Environment, Ecological Index, PSR Framework, Response Indicator, Sentinel-2.

تقييم جودة النظام البيئي في محافظة كركوك و مقاطعة تازة بالاعتماد على طريقة *framework Pressure-State-Response* لشتاء ٢٠٢٣ باستخدام التحسس النائي و نظم المعلومات الجغرافية

سندس محمد عزيز ومنتظر عيدي شريف وفوزي مردان عمر

قسم تقنيات هندسة المساحة\الكلية التقنية الهندسية-كركوك\ الجامعة التقنية الشمالية/ العراق

Sundus.mohammedgs@ntu.edu.iq; Muntadher.a.shareef@ntu.edu.iq; fawzialbeyati@ntu.edu.iq

الخلاصة:

تقييم النظام البيئي لمنطقة ما، هو عامل مهم في تحديد معدل التطور العمراني والتنمية المستدامة. تهدف هذه الدراسة لإيجاد المؤشر البيئي *(EI)* وتقييمه بواسطة الطريقة الشائعة *pressure-state-response (PSR) framework* بالاعتماد على مجموعة من المؤشرات الإحصائية والخاصة بالتحسس النائي في مدينة كركوك ومقاطعة تازة. تم استخدام الصور الفضائية *sentinel-2* للحصول على ١٢ من المؤشرات التي تم صنعها من التحسس النائي لتقييم جودة النظام البيئي. هذه المؤشرات توفر اساساً لصناعة القرار في التنمية المستدامة كتقنية حديثة تدعم التغير الذي يحدث على المدى البعيد من خلال انشاء الخرائط وعرضها تقوم هذه الدراسة بعرض المؤشر البيئي لفصل الشتاء لسنة ٢٠٢٣ في محافظة كركوك ومقاطعة تازة. يشير البحث الى ان الحالة البيئية تبدو أكثر صحة في فصل الشتاء وذلك تبعاً للظروف الجوية والنشاط الاجتماعي والاقتصادي للإنسان بالإضافة الى ان البحث يظهر العلاقة الرئيسية بين الصحة البيئية والنشاط البشري في مختلف الظروف الجوية.

الكلمات المفتاحية: البيئة، المؤشر البيئي، طريقة *PSR*، مؤشر الاستجابة، صور سينتنال-٢.

1. Introduction:

Over the past fifty years, the Ecological Index has become a crucial policy tool for efficient environmental management and pollution control [1]. The region's eco-environmental quality is crucial for sustainable socioeconomic development, ensuring harmony between social production and living environment, and assessing its ability to sustain long-term growth [2]. The natural environment is crucial for the survival and progress of humanity, as it provides vital resources such as water, land, biological resources, and climate [3]. Remote sensing technology is crucial for ecological monitoring in developing countries due to its comprehensive and dynamic compliance with environmental changes [4]. On the other hand, The PSR model highlights the impact of human activities on ecosystem health, including social pressures and resource depletion, highlighting the significant role of human activities [5]. An ecosystem's health status is determined by its vitality, structure, and resilience, while response indicators show how it reacts to changes caused by human activities and the ecosystem itself [6]. Factors like soil temperature, land use, vegetation, heat, soil texture, and aridity influence plant growth, impacting the entire ecosystem if disturbances occur [7]. Changes in land use, such as residential

expansion, can lead to increased environmental conditions. However, manmade and natural factors, such as population growth and economic development, also influence these variations [8]. Land use and cover maps are vital for improving our comprehension of environmental modeling and water management [9]. Theories on health, safety, well-being, residential contentment, and urban environment are derived from historical similar researches and decision-making in urban areas [10]. This study evaluates the eco-environmental system in Kirkuk City and Taza District, focusing on its impact on the impact of human activities and weather condition on the ecological health. It compares five ecological responses in winter 2023, preparing for serious measures.

2. Materials and methods:

2.1. Study area: Figure 1 shows Kirkuk city and Taza District which are situated in the northwestern region of Iraq. It is bordered by the Zagros Mountains to the north, the Hamrin Mountains to the south, the Lower Zab Mountains to the west, and Al-Sulaymaniyah City to the east. Kirkuk City is located at a latitude between 35°13' and 36°29' N and a longitude between 44°00' and 44°50' E. The city has a total size of around 9,679 km2 [11] . The research area experiences a semiarid and Mediterranean climate with hot summers and cold winters, with a heavy precipitation peak from December to March [9]. Temperature plays a significant role in the climate which drops to a low of -1 °C in the winter. The city of Kirkuk is situated in the hilly northern part of the Kirkuk plain, approximately 340-360 meters above sea level.

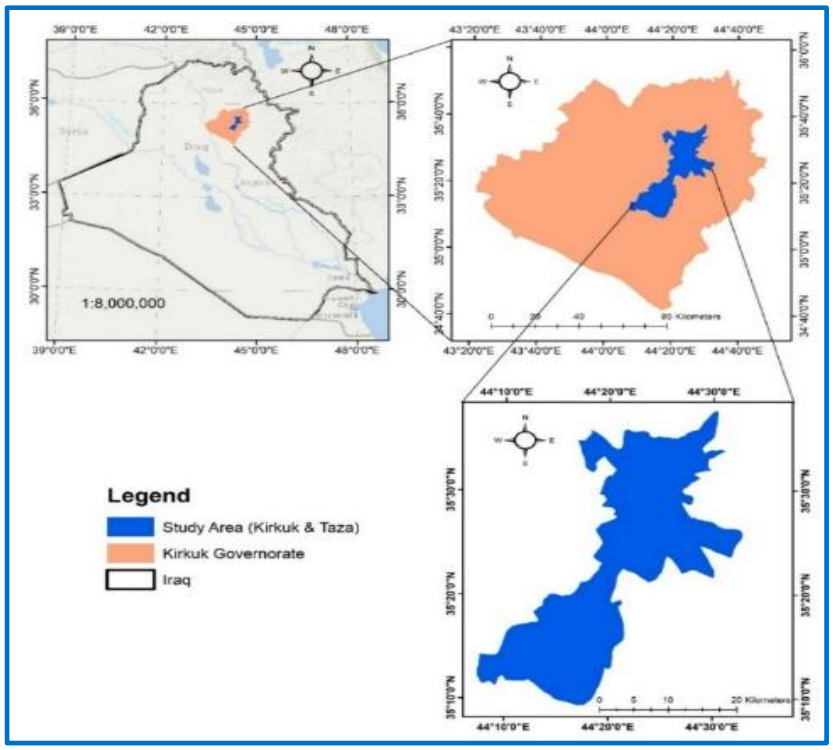

Figure 1: The Study Area of Kirkuk City and Taza District.

2.2. Data and pre-processing

2.2.1. Data used: The study utilized Sentinel-2 data, specifically level-2A images, from a multispectral sensor with 13 channels, ranging from 10 to 60 meters (image details in Table 1). All images were downloaded for free from the Copernicus website (a part of the European Union's space program) with a cloud coverage of less than 2%.

Table 1: Band details of sentinel two satellite image

Bands (wavelength region)	*Central wavelength (nm)*	*Resolution (m)*
Band-1 (coastal aerosol)	443	60
Band-2 (blue)	490	10
Band-3 (green)	560	10
Band-4 (red)	665	10
Band-5 (vegetation red edge)	705	20
Band-6 (vegetation red edge)	740	20
Band-7 (vegetation red edge)	783	20
Band-8 (NIR)	842	10
Band-8A (vegetation red edge)	865	20
Band-9 (water vapour)	945	60
Band-10 (SWIR-Cirrus)	1375	60
Band-11 (SWIR)	1610	60
Band-12 (SWIR)	2190	20

2.2.2. Data Pre-processing: The Bilinear interpolation method was used to resample photos, enhancing their quality and visual appeal. Geometric and atmospheric corrections were not made, as the images are already corrected for surface reflectance. The ortho-images, or granules, have dimensions of 110x110 square kilometers and are projected using the UTM/WGS84 coordinate system as well as registered.

2.3.Methods: The method adopted in this study to obtain the ecological index uses the pressure-state-response (PSR) framework, which utilizes nine indicators to determine the Pressure indicator and three to assess the State indicator. All indicators were obtained using SNAP 9.0.0 software and were output using ArcGIS 10.7 software. The equations were applied using GIS 10.7 software. On the other hand, the Pressure Indicators were including of Digital Elevation Model (DEM), Global Environmental Monitoring Index (GEMI), Land Use/Cover (LULC), Normalized Difference Moisture Index (NDMI), Normalized Difference Water Index (NDWI), Soil Adjusted Vegetation Index (SAVI), Road network and Railway network, Land Surface Temperature (LST). The state indicators were included from Fractional Vegetation Cover (FVC), Normalized Leaf Area Index (LAI), and Normalized Difference Vegetation Index (NDVI). To ensure that each indication has a comparable weight and significance in the outcome, all indicators were rescaled and normalized from 0 to 1. The overall methodology is explained in Figure 2.

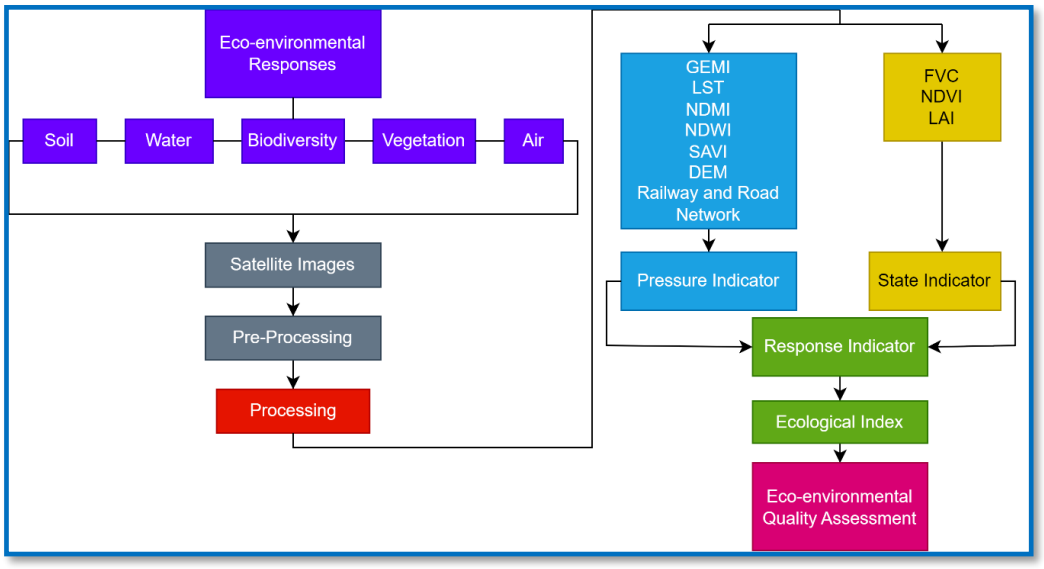

Figure 2: The Overall Methodology

2.3.1. Indicators used:

1. Global Environmental Monitoring Index (GEMI): GEMI is a nonlinear vegetation index derived from satellite data used for global environmental monitoring, more resistant to atmospheric influences than NDVI, ranging from 0 to 1, where 0 indicates the absence of plant cover and 1 indicates complete vegetation c(2.3over on the ground [12]. **Figure 3** shows the GEMI.
2. Fractional vegetation cover (FVC): is a crucial measure for understanding soil erosion, climate change, and ecosystem balance. It measures plant arrangement on Earth's surface, ranging from 0 to 1, with 0 indicating no vegetation and 1 indicating complete cover [13]. **Figure 4** shows the obtained FVC.
3. Leaf Area Index (LAI): is a dimensionless number used to characterize plant canopies, ranging from 0 to 10, indicating the presence of dense conifer forests [14]. **Figure 5** shows the LAI.
4. Normalized Difference Moisture Index (NDMI): This index is not standardized. The index, ranging from -1 to 1, is easily comprehensible and indicates a higher level of vegetation health and density [15]. The dry matter content of leaves is highly correlated with the NDMI indices [16]. **Figure 6** shows the NDMI.
5. Normalized Difference Vegetation Index (NDVI): Sensor data is used to measure plant density and health, with values ranging from -1 to 1, indicating greater vegetation abundance and density [15]. The index reduces or deletes characteristics with low red light and near-infrared reflectance, like water, while amplifying those with high NIR reflectance and lower red light reflectance, like terrestrial vegetation [17]. **Figure 7** shows the NDVI.

6.Normalized Difference Water Index (NDWI): Sensor data quantifies vegetation density and health using near-infrared and red wavelengths. Higher values indicate healthier vegetation. NDWI can provide information on liquid water content, although spectrum-matching techniques aren't suitable for determining vegetation water content [18]. **Figure 8** shows the NDWI.

7. Railway and road network: Human activity impacts ecosystems by examining road and rail networks, infrastructure, and utility systems. Increased modifications indicate higher frequency of activity. Population density correlates with larger roads, facilitating more frequent transportation. Road data in the research region includes primary, secondary, residential, and local roadways [7]. The increase in traffic brought on by projects could be offset by further highway funding [19]. The estimated railway and road networks are shown in **Figure 9**, where (A) is the road network map and (B) is the railway network map.

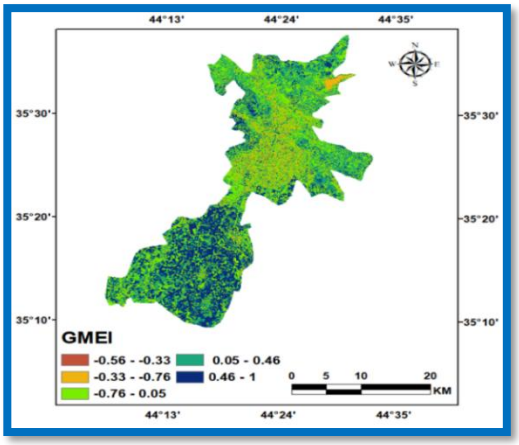

Figure 3: GEMI of Winter 2023.

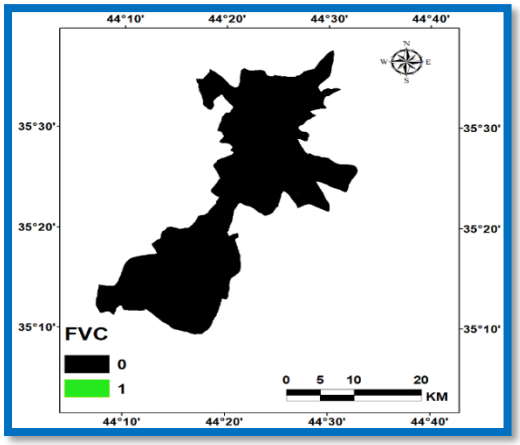

Figure 4: FVC of Winter 2023.

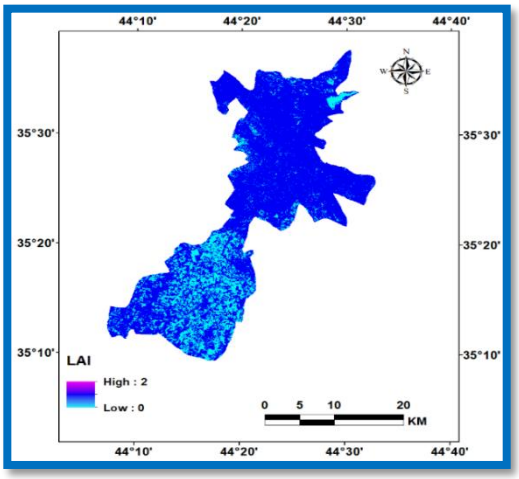

Figure 5: LAI of Winter 2023.

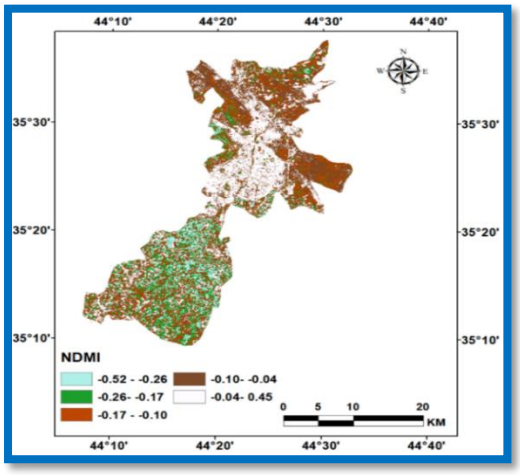

Figure 6: NDMI of Winter 2023.

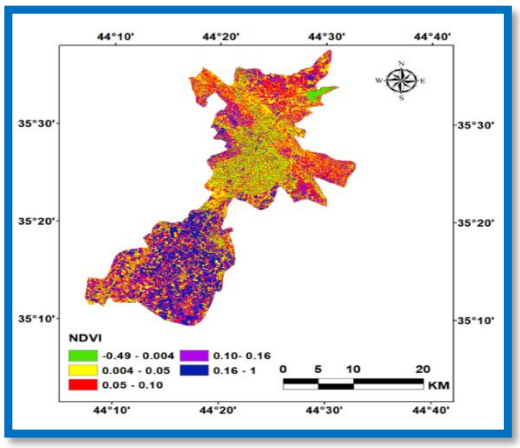

Figure 7: NDVI of Winter 2023.

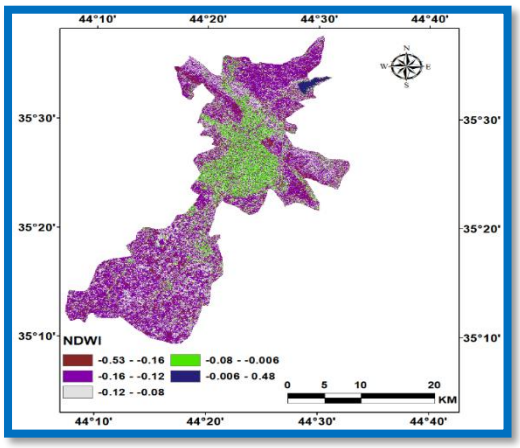

Figure 8: NDWI of Winter 2023.

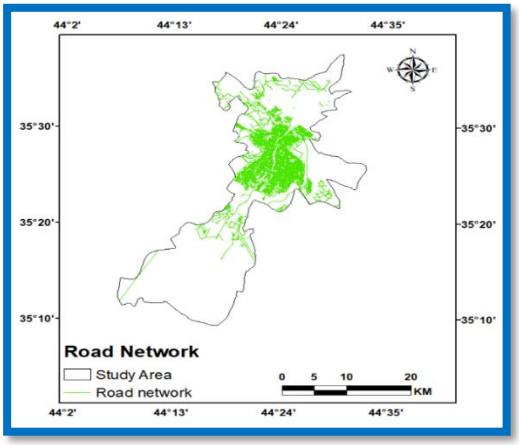

(A) Road network

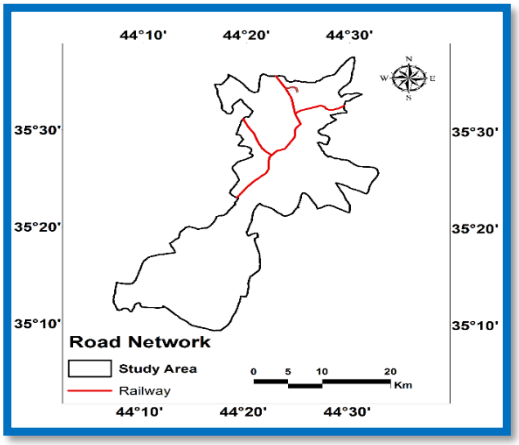

(B) railway network

Figure 9: Road Network and Railway Network

8.Land Use/Land Cover: Accurate land use and land cover data is crucial for urban planning, decision-making, population dynamics, and public health assessment [20]. Assessing land use and vegetation cover is crucial for urban planning and policy formulation due to growing structures and population spread in metropolitan areas [21]. Land inventories involve land use and land cover, crucial in climate models. Land use describes ecosystem function, social, economic, and cultural utility, requiring analysis of socioeconomic activities in the location [22]. The Support Vector Machine (SVM) classification method was used to obtain classes represented by urban areas, water bodies, barren areas, agricultural areas, and vegetation. The classification is shown in **Figure 10**.

9.Soil-Adjusted Vegetation Index (SAVI): Land inventories involve land use and land cover, crucial in climate models. Land use describes ecosystem function, social, economic, and cultural utility, requiring analysis of socioeconomic activities in the location [23]. It has significantly improved the development of global models that accurately describe dynamic soil-vegetation systems using remotely sensed data [24]. **Figure 11** shows the SAVI.

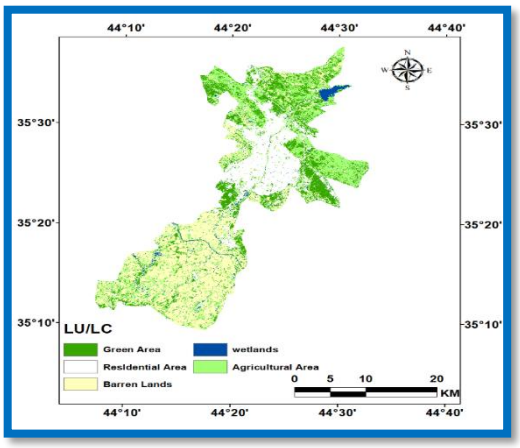

Figure 10: LULC of Winter 2023.

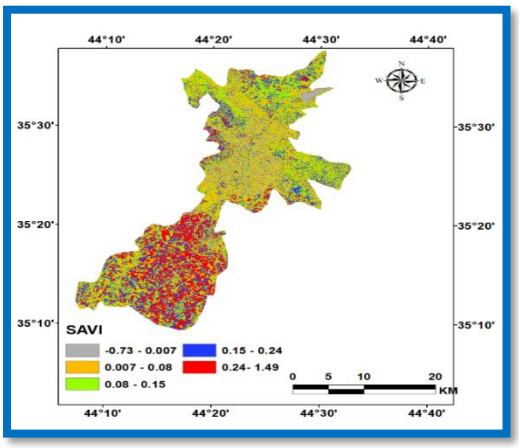

Figure 11: SAVI of Winter 2023.

10 . Digital Elevation Model (DEM): A digital elevation model (DEM) is a crucial spatial resource in GIS, representing terrain through a collection of digital data indicating ground elevation (spot height) [25]. Topography significantly impacts water balance in catchments, affecting surface and subsurface runoff, water movement, and routes. Fully distributed hydraulic and hydrological models use topography, represented by the Digital Elevation Model, to establish bathymetry [26]. The DEM that was used in this study is represented in Figure 12.

11. Land Surface Temperature (LST): Remotely sensed land surface temperature (LST) is intriguing for biological and environmental purposes due to challenges in weather observatories, field surveys, and data interpolation [27]. Land surface temperature (LST) is a crucial parameter in land-surface models, influencing turbulent heat exchanges and long-wavelength radiation at the ground-atmosphere interface, affecting aridity, soil moisture, and evapotranspiration [28]. It is directly correlated with the development and distribution of vegetation and the cycle of evaporation of surface water resources [29]. Figure 13 shows the obtained LST.

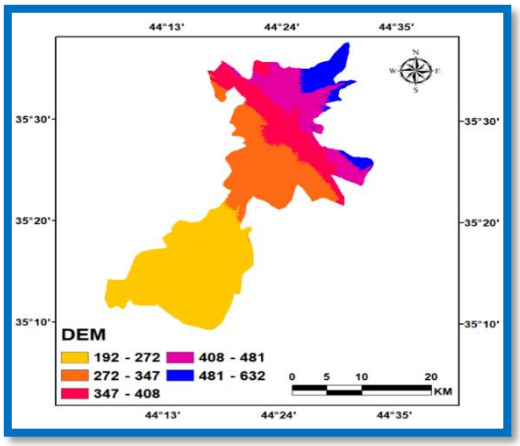

Figure 12: Digital Elevation Model (in meters) of Kirkuk City and Taza District

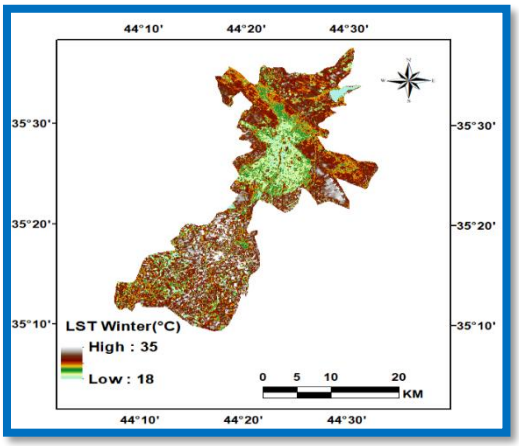

Figure 13: LST of Winter 2023.

2.3.2. PSR framework: The Pressure-State-Response concept explains how human activities impact the environment, providing more comprehensive information than two-dimensional indicator sets, using three categories: Pressure Indicator, State Indicator, and Response Indicator [30]. The dynamic and systematic interactions between the economic, social, and ecological environments can be reflected in the three dimensions of the PSR framework [31]. Depending on the concerns or progress that need to be looked at, a PSR framework's indicators can be chosen accordingly. There wouldn't be a standard set of indicators, and the choices might differ depending on the nation or the location. Data accessibility is still another crucial factor [32].

2.3.2.1. Pressure indicator (PI): Human activity's impact on ecosystem health is described using pressure indicators like social and resource demands [33]. the PI value from standardized data ranges from 0 to 1, giving each indicator in the research region equal weight, as shown in Eq. (1) [7].

$$PI = \frac{GEMI + SAVI + NDMI + LULC + Road + Rail + LI + NDWI + DEM}{9} \quad (1)$$

2.3.2.2. State indicator (SI): State indicators accurately represent an ecosystem's current health status by assessing its robustness, structure, and adaptability [33]. Healthy natural phenomena, such as NDVI, LAI, FVC, forests, mangroves, wetland wetlands, and waterbodies, are generally indicative of healthy ecosystems. All parameters were first standardized from a range of 0 to 1 and then given equal weight as per Eq. (2) to generate the state indicator. Higher SI values suggest improved ecological circumstances, while lower values indicate deteriorating ecological conditions [7].

$$SI = \frac{(NDVI + LAI + FVC)}{3} \quad (2)$$

2.3.2.3. Response indicator (RI): Response indicators depict an ecosystem's response to changes in its overall well-being, encompassing human activities and internal processes [33]. Response indicators indicate high-pressure conditions, indicating ecological disruption, while low reaction indicators suggest stable conditions with minimal changes due to lower demand, indicating sustainable development and controlled ecology, contrasting with elevated reactions suggesting significant environmental changes. RI can be calculated from the Eq. (3) [7].

$$RI = PI - SI \quad (3)$$

2.3.2.4. Calculation of EI: The ecological index significantly influences ecological quality assessment due to its consistency with average values within intervals, and normalizing it during calculation is crucial due to inconsistent dimensions [34]. EI can be calculated from Eq.

(4), where EI is an ecological indicator, and w and c represent the weight and standardized data [7].

$$EI = \sum_{i=1}^{n} W * C \quad (4)$$

By using all the ecological response parameters, the ecological indicator was calculated in this paper from Eq. (5).

$$EI = w(environment) + w(climate) + w(soil\ moisture) + w(greenness) + w(LCLU) + w(artificial\ features\ \&\ energy) + w(water\ content) + w(landscape) \quad (5)$$

Where the Environmental parameter refers to the global environmental monitoring index (GEMI); Climate parameter: Soil moisture: soil adjusted vegetation index (SAVI) and normalized difference moisture index (NDMI); Greenness: normalized difference vegetation index (NDVI), leaf area index (LAI), fractional vegetation cover (FVC); Land use/land cover: LULC change; Artificial features and energy: Road network, Railway network; Water content: normalized difference water index (NDWI); Landscape: digital elevation model (DEM).

The study analyzes the Eco-environmental quality assessment (EEQ) using the pressure-state-response (PSR) approach and describes the Ecological Index (EI) of winter 2023.

3. Results:

3.1.General assessment of PSR

3.1.1. Pressure indicator: The PI is a measure of atmospheric pressure in urbanized areas, with high levels observed in developed areas. The central region of Kirkuk city experiences high pressure, while surrounding villages experience mild pressure due to lower socio-economic activities. The PI is positively correlated with population size and negatively correlated when population decreases as shown in Figure 14.

3.1.2. State indicator: The SI is mostly derived from the measurements of FVC, NDVI, and LAI. As a result of the humid winters in Kirkuk City, the vegetation was in excellent condition. The southwestern portion of the research region has dense vegetation, resulting in comparatively higher NDVI values towards the south. Given that both FVC and LAI serve as indicators of robust vegetation, they exhibited a similar NDVI pattern. The ultimate SI map, depicted in Figure 15, exhibits the combined influence of all vegetative indices. The SI exhibits consistently high values in both seasons.

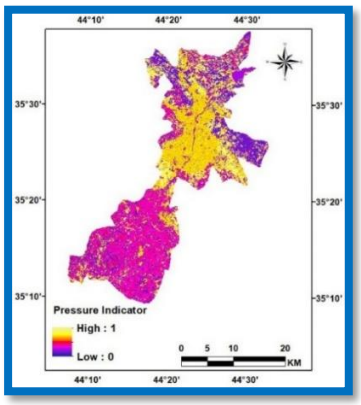

Figure 14: PI of Winter 2023.

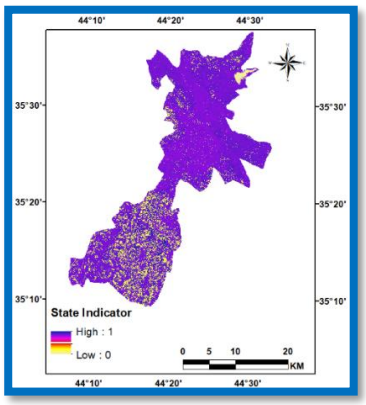

Figure 15: SI of Winter 2023.

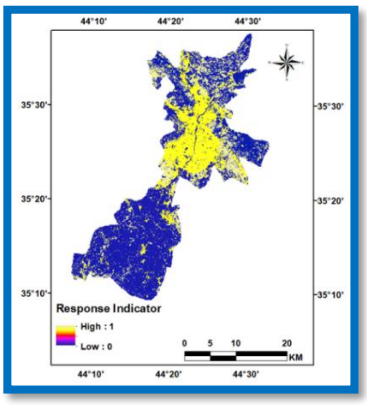

Figure 16: RI of Winter 2023.

3.1.3. Response indicator: Under significant anthropogenic strain, ecological conditions that are weaker, unhealthy, and unstable are indicated by strong reaction indicators, and conversely. Elevated RI values are symptomatic of heightened natural/human pressure and socioeconomic activity, such as industrial expansion, farming, and urban growth, which can lead to ecological disruption. Low RI values indicate less human involvement in ecosystems, including green fields, aquatic bodies, and remote areas far from metropolitan centers. According to the RI maps, the ecological status is consistently progressing, as seen in **Figure 16**. The study suggests that the southern part of the area possesses more favorable ecological traits in comparison to its central section. The data suggests that the resilience index (RI) for the agriculture and cultivation sectors was lower compared to the RI for socioeconomic activity locations.

3.2. Ecological Index: Elevated EI levels imply an ecological ecosystem that is strong and expanding, while lower values indicate the opposite. **Figure 17** shows a study region with a moderate to high EI value. The northeastern and eastern areas of the research region exhibit slightly superior conditions compared to other sections, as they display the greatest values concentrated around Khasa and in close proximity to Sulaymaniyah city towards the east. Human activity intensifies in the center region of the study area. Consequently, the central area of Kirkuk City has the lowest values spread out over a significant distance. The southern and southwestern regions of the research area, where Taza is situated, exhibit a moderate EI value, as depicted in Figure 17. The spatial distribution of EI maps indicates that the regions in close proximity to water bodies had exceptional EI conditions, while the adjacent area displayed a range of EI conditions from excellent to moderate. There were several industrial and residential regions characterized by suboptimal ecological conditions. The northern part of the research area has a high level of ecological condition, ranging from good to exceptional. In contrast, the southern part of the area shows a moderate level of ecological condition, ranging from good to

acceptable. Table 2 displays assessments and their respective regions derived from Figure 17. In contrast to the Taza district, the central area of the research region and Kirkuk City exhibit ecological conditions ranging from fair to bad. This highlights the urgent need for an intervention by a responsible and responsive ethics commission to address this significant problem.

Table 2: Evaluations and their Corresponding Areas.

Evaluation	*Corresponding area (km^2)*
Extreme excellent – excellent	229.3
Excellent – good	142.5
Good – fair	165.93
Fair – poor	97.36
Poor – bad	44.65

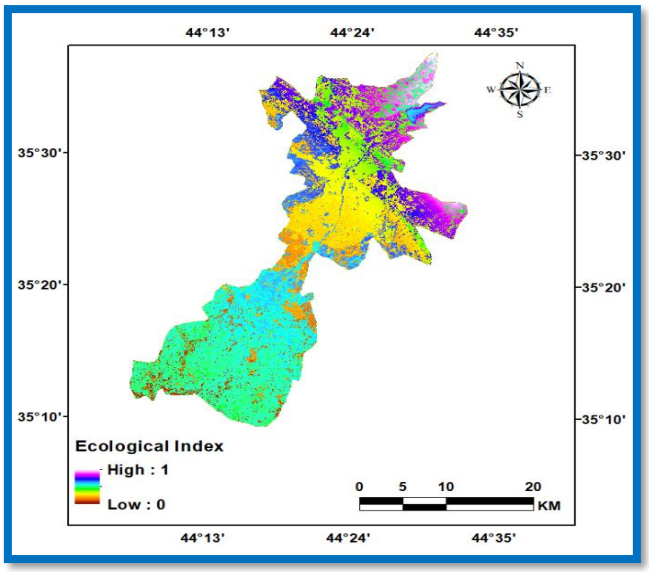

Figure 17: EI of Winter 2023.

4. Discussion

This research aims to identify and measure the ecological index to support the Environmental Quality Evaluation (EEQ) in Kirkuk City, Iraq. The Environmental Index (EI) is considered the most precise measure for evaluating the environmental state. GIS and remote sensing technologies are used to monitor environmental quality in areas like Kirkuk City, Iraq. The study uses time series remote sensing satellite data and the PSR framework to develop 12 indicators related to environmental concerns. The assessment considers land use/cover change, human and natural pressure, the environment's condition, and ecosystem health. The study also examines the role of the vegetative ecosystem in reducing pressure indicators and protecting the environment. The study identifies areas that have been safeguarded by the government to conserve the environment and minimize human activities. The findings are significant for

NGOs, government policymakers, and individuals interested in sustainable development due to their wide-ranging applications.

5. Conclusions

This research utilizes GIS and remote sensing data to assess the eco-environmental status. It achieves this by calculating the primary ecological indicators within the PSR framework in order to control the EEQ. The EI effectively evaluates the condition of the study region by employing a range of indicators that measure different influences on the environmental system. The study identifies that dryness and high temperatures have detrimental effects on the environment, while indicators of greenness and wetness have a positive impact. The improvement in EEQ (Environmental Quality Index) is dependent on the positive values observed in natural responses. Human activity, especially social and economic activities, significantly impacts the ecological health by causing harm to the system.

6. References

[1] X. Wang, Y. Cao, X. Zhong, and P. Gao, "A New Method of Regional Eco-environmental Quality Assessment and Its Application," *J. Environ. Qual.*, vol. 41, no. 5, pp. 1393–1401, 2012, doi: 10.2134/jeq2011.0390.

[2] H. Ma and L. Shi, "Assessment of eco-environmental quality of Western Taiwan Straits Economic Zone," *Environ. Monit. Assess.*, vol. 188, no. 5, 2016, doi: 10.1007/s10661-016-5312-5.

[3] A. M. Duda and M. T. El-Ashry, "Addressing the global water and environment crises through integrated approaches to the management of land, water and ecological resources," *Water Int.*, vol. 25, no. 1, pp. 115–126, 2000, doi: 10.1080/02508060008686803.

[4] J. Li, Y. Pei, S. Zhao, R. Xiao, X. Sang, and C. Zhang, "A review of remote sensing for environmental monitoring in China," *Remote Sens.*, vol. 12, no. 7, pp. 1–25, 2020, doi: 10.3390/rs12071130.

[5] S. Das, B. Pradhan, P. K. Shit, and A. M. Alamri, "Assessment of wetland ecosystem health using the pressure-state-response (PSR) model: A case study of Mursidabad District of West Bengal (India)," *Sustain.*, vol. 12, no. 15, 2020, doi: 10.3390/SU12155932.

[6] J. Xiong, W. Li, H. Zhang, W. Cheng, C. Ye, and Y. Zhao, "Selected environmental assessment model and spatial analysis method to explain correlations in environmental and socio-economic data with possible application for explaining the state of the ecosystem," *Sustain.*, vol. 11, no. 17, 2019, doi: 10.3390/su11174781.

[7] M. S. Boori, K. Choudhary, R. Paringer, and A. Kupriyanov, "Eco-environmental quality assessment based on pressure-state-response framework by remote sensing and GIS," *Remote Sens. Appl. Soc. Environ.*, vol. 23, no. April, p. 100530, 2021, doi: 10.1016/j.rsase.2021.100530.

[8] R. Sun *et al.*, "Effects of land-use change on eco-environmental quality in Hainan Island, China," *Ecol. Indic.*, vol. 109, no. 4, p. 105777, 2020, doi: 10.1016/j.ecolind.2019.105777.

[9] M. A. Shareef, N. D. Hassan, S. F. Hasan, and A. Khenchaf, "Integration of sentinel-1A and sentinel-2B data for land use and land cover mapping of the Kirkuk governorate, Iraq," *Int. J. Geoinformatics*, vol. 16, no. 3, pp. 87–96, 2020.

[10] M. Pacione, "Urban environmental quality and human wellbeing - A social geographical perspective," *Landsc. Urban Plan.*, vol. 65, no. 1–2, pp. 19–30, 2003, doi: 10.1016/S0169-2046(02)00234-7.

[11] V. F. Salahalden, M. A. Shareef, and Q. A. A. Nuaimy, "Red Clay Soil Physical and Chemical Properties Distribution Using Remote Sensing and GIS Techniques in Kirkuk City, Iraq," *Iraqi Geol. J.*, vol. 57, no. 1, pp. 194–220, 2024, doi: 10.46717/igj.57.1A.16ms-2024-1-27.

[12] A. B. Pinty, M. M. Verstraete, S. Vegetatio, N. Jul, and B. Pinty, "GEMI : A Non-Linear Index to Monitor Global Vegetation from Satellites GEMI : a non-linear index to monitor global vegetation from satellites," *Vegetatio*, vol. 101, no. 1, pp. 15–20, 2011.

[13] D. Chu, *Fractional vegetation cover, or FVC, is a crucial metric in the study of soil erosion, climate change, and ecosystem balance. It is frequently employed in the assessment and tracking of vegetation degradation and desertification. The only practical method*. 2019. doi: 10.1007/978-981-13-7580-4.

[14] H. Fang, F. Baret, S. Plummer, and G. Schaepman-Strub, "An Overview of Global Leaf Area Index (LAI): Methods, Products, Validation, and Applications," *Rev. Geophys.*, vol. 57, no. 3, pp. 739–799, 2019, doi: 10.1029/2018RG000608.

[15] S. Rahman and V. Mesev, "Change vector analysis, tasseled cap, and NDVI-NDMI for measuring land use/cover changes caused by a sudden short-term severe drought: 2011 Texas event," *Remote Sens.*, vol. 11, no. 19, 2019, doi: 10.3390/rs11192217.

[16] O. Strashok, M. Ziemiańska, and V. Strashok, "Evaluation and Correlation of Sentinel-2 NDVI and NDMI in Kyiv (2017-2021)," *J. Ecol. Eng.*, vol. 23, no. 9, pp. 212–218, 2022, doi: 10.12911/22998993/151884.

[17] S. K. McFeeters, "NDWI BY McFEETERS," *Remote Sens. Environ.*, vol. 25, no. 3, pp. 687–711, 1996.

[18] X. Wang, Y. Yan, and Y. Cao, "Impact of historic grazing on steppe soils on the northern Tibetan Plateau," *Plant Soil*, vol. 354, no. 1–2, pp. 173–183, 2012, doi: 10.1007/s11104-011-1053-y.

[19] A. C. Neri, P. Dupin, and L. E. Sánchez, "A pressure-state-response approach to cumulative impact assessment," *J. Clean. Prod.*, vol. 126, no. April, pp. 288–298, 2016, doi: 10.1016/j.jclepro.2016.02.134.

[20] S. F. Hasan, M. A. Shareef, and N. D. Hassan, "Speckle filtering impact on land use/land cover classification area using the combination of Sentinel-1A and Sentinel-2B (a case study of Kirkuk city, Iraq)," *Arab. J. Geosci.*, vol. 14, no. 4, 2021, doi: 10.1007/s12517-021-06494-9.

[21] M. A. Shareef, M. H. Ameen, and Q. M. Ajaj, "Change detection and gis-based fuzzy ahp to evaluate the degradation and reclamation land of tikrit city, Iraq," *Geod. Cartogr.*, vol. 46, no. 4, pp. 194–203, 2020, doi: 10.3846/gac.2020.11616.

[22] A. Comber and M. Wulder, "Considering spatiotemporal processes in big data analysis: Insights from remote sensing of land cover and land use," *Trans. GIS*, vol. 23, no. 5, pp. 879–891, 2019, doi: 10.1111/tgis.12559.

[23] P. P. Rhyma, K. Norizah, O. Hamdan, I. Faridah-Hanum, and A. W. Zulfa, "Integration of normalised different vegetation index and Soil-Adjusted Vegetation Index for mangrove vegetation delineation," *Remote Sens. Appl. Soc. Environ.*, vol. 17, no. December 2019, p. 100280, 2020, doi: 10.1016/j.rsase.2019.100280.

[24] A. R. Huete, "A soil-adjusted vegetation index (SAVI)," *Remote Sens. Environ.*, vol. 25, no. 3, pp. 295–309, 1988, doi: 10.1016/0034-4257(88)90106-X.

[25] Q. Zhou, "Digital Elevation Model and Digital Surface Model," *Int. Encycl. Geogr.*, no. March, pp. 1–17, 2017, doi: 10.1002/9781118786352.wbieg0768.

[26] J. Vaze, J. Teng, and G. Spencer, "Impact of DEM accuracy and resolution on topographic indices," *Environ. Model. Softw.*, vol. 25, no. 10, pp. 1086–1098, 2010, doi: 10.1016/j.envsoft.2010.03.014.

[27] M. Neteler, "Estimating daily land surface temperatures in mountainous environments by reconstructed MODIS LST data," *Remote Sens.*, vol. 2, no. 1, pp. 333–351, 2010, doi: 10.3390/rs1020333.

[28] G. C. Hulley, D. Ghent, F. M. Göttsche, P. C. Guillevic, D. J. Mildrexler, and C. Coll, *Land Surface Temperature*. 2019. doi: 10.1016/B978-0-12-814458-9.00003-4.

[29] W. Ren, X. Zhang, and H. Peng, "Evaluation of Temporal and Spatial Changes in Ecological Environmental Quality on Jianghan Plain From 1990 to 2021," *Front. Environ. Sci.*, vol. 10, no. May, pp. 1–14, 2022, doi: 10.3389/fenvs.2022.884440.

[30] B. Wolfslehner and H. Vacik, "Evaluating sustainable forest management strategies with the Analytic Network Process in a Pressure-State-Response framework," *J. Environ. Manage.*, vol. 88, no. 1, pp. 1–10, 2008, doi: 10.1016/j.jenvman.2007.01.027.

[31] J. Ji and J. Chen, "Urban flood resilience assessment using RAGA-PP and KL-TOPSIS model based on PSR framework: A case study of Jiangsu province, China," *Water Sci. Technol.*, vol. 86, no. 12, pp. 3264–3280, 2022, doi: 10.2166/wst.2022.404.

[32] H. F. Huang, J. Kuo, and S. L. Lo, "Review of PSR framework and development of a DPSIR model to assess greenhouse effect in Taiwan," *Environ. Monit. Assess.*, vol. 177, no. 1–4, pp. 623–635, 2011, doi: 10.1007/s10661-010-1661-7.

[33] D. Liu and S. Hao, "Ecosystem health assessment at county-scale using the pressure-state-response framework on the loess plateau, China," *Int. J. Environ. Res. Public Health*, vol. 14, no. 1, 2017, doi: 10.3390/ijerph14010002.

[34] R. Sensing and E. Index, "Evaluation of the Spatiotemporal Variations in the Eco-environmental Quality in China Based on the Remote Sensing Ecological Index," *Remote Sens.*, 2020.